science, engineering and health studies

Research Article

Science, Engineering and Health Studies
https://lio1.tci-thaijo.org/index.php/sehs
ISSN (Online): 2630-0087

Synthesis of chitosan-graft-methacrylate with enhanced antimicrobial activity for improved mucoadhesive properties and controlled drug delivery systems

Peerapat Chidchai[1], Shoon Lai Thaw Tar Aung[2], Kanokwan Singpanna[1], Praneet Opanasopit[1] and Chaiyakarn Pornpitchanarong[1]*

[1] Pharmaceutical Development of Green Innovations Group (PDGIG), Faculty of Pharmacy, Silpakorn University, Nakhon Pathom 73000, Thailand
[2] University of Pharmacy, Mandalay-Lashio Rd, Mandalay 05032, Republic of the Union of Myanmar

***Corresponding author**: Chaiyakarn Pornpitchanarong pornpitchanaron_c@su.ac.th*

***Received**: 18 April 2023*
***Revised**: 18 May 2023*
***Accepted**: 23 May 2023*
***Published**: 26 September 2023*

***Citation**: Chidchai, P., Aung, S. L. T. T., Singpanna, K., Opanasopit, P., and Pornpitchanarong, C. (2023). Synthesis of chitosan-graft-methacrylate with enhanced antimicrobial activity for improved mucoadhesive properties and controlled drug delivery systems. Science, Engineering and Health Studies, 17, 23050004.*

ABSTRACT

Chitosan (CS) is a derivative of chitin that displays antimicrobial effects and has other attributes that make it of interest for use in a variety of applications, including drug delivery systems. This study aimed to synthesize chitosan-graft-methacrylate (CS-g-MA) to improve the antimicrobial activities of CS for use in controlled drug delivery systems. CS-g-MA was synthesized via a nucleophilic acyl substitution reaction by gradually adding methacrylic anhydride (MA) to a CS solution until the ratio of CS to MA achieved the maximum degree of substitution. Proton nuclear magnetic resonance spectroscopy and attenuated total reflection-Fourier transformed infrared spectroscopy were used to characterize the resulting polymer. Its mucoadhesive capabilities and cytotoxicity toward human fibroblasts were evaluated, as well as its antimicrobial activities against *Staphylococcus aureus*, *Escherichia coli*, and *Candida albicans* using the minimum inhibitory concentration and minimum bactericidal concentration tests. The optimized CS-g-MA polymer had an optimal weight CS:MA ratio of 3:4 and was combined with sodium fluorescein in tablet form to evaluate drug release. CS-g-MA improved the mucoadhesive capabilities of CS by increasing the number of intermolecular interactions with the grafted moiety. CS-g-MA was non-toxic to normal human fibroblasts and exhibited superior efficacy against *S. aureus, E. coli,* and *C. albicans* compared to CS. Furthermore, the CS-g-MA tablet regulated drug release for an extended period of more than 72 h. Thus, CS-g-MA shows significant potential for further development in advanced drug delivery systems.

Keywords: chitosan; methacrylic anhydride; antimicrobial activity

1. INTRODUCTION

Chitosan (CS) is a biopolymer derived from chitin that is composed of D-glucosamine and *N*-acetyl-D-glucosamine. The cationic nature of CS makes it an attractive material for various applications. Its biocompatibility, biodegradability, nontoxicity, and mucoadhesive properties make it a promising candidate for drug delivery and tissue engineering. Additionally, CS can inhibit the growth of microorganisms, such as bacteria and fungi, which makes it a promising natural substitute for synthetic antimicrobial agents (Kolawole et al., 2018; Kumar et al., 2004; Shariatinia, 2019). Due to its numerous advantages, CS is a good candidate for application in various fields, including pharmaceuticals,

food, cosmetics, chemicals, and agricultural crops. CS is soluble in acidic conditions, but has a poor solubility in neutral and basic conditions, which limits its use (Aranaz et al., 2021). Chemical modifications can be made to the structure of CS to enhance its performance by improving its mucoadhesive properties, its ability to control drug release, and its antimicrobial and antifungal activities (Cankaya, 2019). Above all, CS has become a versatile material for numerous biomedical applications (Ke et al., 2021; Kenawy et al., 2016; Kolawole et al., 2018).

Global public health has been significantly impacted by infectious diseases during the last decade. Serious illnesses can be caused by exposure to microorganisms or their toxins via airborne transmission, ingestion, or dermal infection (Deusenbery et al., 2021). CS can inhibit a wide range of microorganism growth, from gram-positive and gram-negative bacteria to yeasts and molds. (Kongkaoroptham et al., 2021; Shanmugam et al., 2016). The amino groups of the CS structure generate a positive charge through protonation and are primarily responsible for its antimicrobial actions (Matica et al., 2019; Xing et al., 2014). Specifically, its antimicrobial and antifungal activities are produced by the electrostatic interaction between the cationic CS and the anionic microbe surface, which results in the disruption of the cell membrane or cell wall and the release of intracellular components.

Acylation is the most frequently used method to modify the CS structure and occurs when CS reacts with different organic acids. The obtained derivatives are known as acylations of CS (i.e., mainly anhydride and acyl chloride; Wang et al., 2020). These CS derivatives have gained significant interest due to their potential to tailor the physicochemical and biological properties of CS to suit various applications. Among the different reagents used for acylation, methacrylic anhydride (MA) has emerged as a promising candidate since it is capable of grafting onto the CS structure without a crosslinker. This minimizes the use of chemical reagents, making the reaction process simpler and more efficient (Kolawole et al., 2018). The resulting conjugation of chitosan-*graft*-methacrylate (CS-g-MA) has been shown to enhance the biocompatibility and improve the solubility of CS in aqueous media via increased hydrophilicity (Sogias et al., 2010).

MA is a liquid that ranges from colorless to light yellow or light orange. It has a molecular weight of 154.16 Da and is commonly used to prepare various types of monomers in light-curing coatings and when cross-linking polymers (Wang et al., 2014). The methacryloyl moieties of MA can be utilized through covalent bonding with certain organic compounds that contain hydroxyl and amino groups. These modified compounds can be used in polymerization or reactions involving thiols (Yu et al., 2007). The chemical structure of CS (Figure 1) possesses an amino group that can be grafted to the methacryloyl of MA to form CS-g-MA. Its stronger attachment to the thiol functional groups of mucins allows CS-g-MA to have greater mucoadhesive properties (Kolawole et al., 2018).

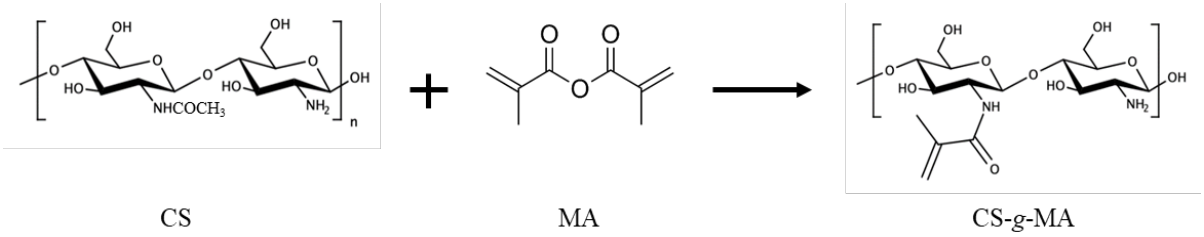

Figure 1. The synthesis scheme of CS-g-MA

Numerous studies have demonstrated the efficacy of drug delivery systems that utilize CS to protect their therapeutic agents from the degradation caused by acid and gastric enzymes (Das et al., 2022). Delivery systems that use CS can increase the duration that drugs remain in the gastrointestinal tract and improve drug absorption through the intestinal lining. The unique functional groups of CS can be modified to attain various desired outcomes, which makes it is a versatile polymer in pharmaceutical and biomedical applications. CS-based delivery systems have been extensively used for the oral administration of therapeutic agents, including anti-infectives, anticancer drugs, peptides, proteins, genes, nucleic acids, and vaccines (Bernkop-Schnürch and Dünnhaupt, 2012). Thus, CS and its derivatives are promising candidates for the development of oral drug delivery systems (Siti Zuhairah and Khuriah Abdul, 2021).

The aim of this study was to improve and optimize the physicochemical properties, antimicrobial activities, and mucoadhesive capabilities of CS in a controlled drug delivery platform by developing and testing CS-g-MA using various MA to CS ratios. The optimal ratio was selected based on the degree of substitution (DS) and product yield. The selected CS-g-MA polymer was mixed with a model drug (sodium fluorescein; SFC) in tablet form to assess its drug release rates and demonstrate its use as a drug delivery platform. In addition, the antibacterial and antifungal activities of the polymer were examined using *Staphylococcus aureus*, *Escherichia coli*, and *Candida albicans* to represent gram-positive bacteria, gram-negative bacteria, and fungi, respectively.

2. MATERIALS AND METHODS

2.1 Materials

CS (low molecular weight of 50–190 kDa; 75%–85% deacetylated), MA, and SFC were purchased from Sigma Aldrich (St. Louis, MO, USA). Acetic acid-D4 and deuterium oxide (D_2O) were procured from Cambridge Isotope Laboratories (Massachusetts, US). Nutrient and Sabouraud dextrose broth and agar were bought from Millipore (Darmstadt, Germany). L-glutamine, nonessential amino acids, penicillin-streptomycin, fetal bovine serum (FBS), and Dulbecco's modified Eagle's medium (DMEM) were acquired from Thermo Fisher Scientific (Massachusetts, US). Normal human fibroblasts were purchased from American Type Culture Collection (ATCC®, VA, USA). All other solvents and chemicals were used as received without purification.

2.2 Synthesis of CS-g-MA

CS-g-MA was synthesized at various weight ratios (1.5:4; 3:4; and 4.5:4; Table 1) using a modified version of the method by Kolawole et al. (2018). Briefly, CS was dissolved in 100 mL of 0.2 N hydrochloric acid (HCl) in a round-bottomed flask and stirred overnight to ensure complete dissolution. Next, MA was slowly added in a dropwise manner to the CS solution, which was then purged with nitrogen (N_2) gas and stirred at room temperature for 12 h to allow the reaction between the two components to occur. Once the reaction was complete, the resulting solution was transferred into a dialysis bag with a molecular weight cut-off of 3.5 kDa and dialyzed with deionized water for 3 days. During dialysis, the solution was discarded and replaced with deionized water every 6 h to ensure that the resulting polymer was completely purified. Finally, the polymer solution was frozen at −20 °C overnight and placed in a freeze dryer (Christ, Germany) to obtain the polymer in its dried form.

2.3 Characterization of CS-g-MA

2.3.1 ^{1}H-Nuclear magnetic resonance spectroscopy

Approximately 5 mg of CS, MA, and CS-g-MA were subjected to ^{1}H-nuclear magnetic resonance spectroscopy (^{1}H NMR; 300 MHz Advance III HD, Bruker) to ensure an in-depth understanding of the polymers' molecular architecture was obtained. ^{1}H NMR was performed at 298 MHz with 1% acetic acid-D_4 in deuterium oxide (D_2O) as the solvent. The chemical shift value was expressed as parts per million (ppm). In addition, the D_2O chemical shift acted as a reference point and was determined at precisely 4.80 ppm.

2.3.2 Degree of substitution

The DS in CS-g-MA was determined by analyzing the average number of methacrylate groups attached per base unit of CS using ^{1}H NMR. The DS value of CS-g-MA was calculated using Equation 1.

$$\% \text{ DS} = \frac{(A/2)}{(B/7)} \times 100 \qquad (1)$$

where, A is the integral of methacrylate protons and B is the integral of the pyranose protons of chitosan.

2.3.3 Attenuated total reflectance Fourier transform infrared spectroscopy

Attenuated total reflectance Fourier transform infrared spectroscopy (ATR-FTIR; Nicolet iS5; Thermo Fisher Scientific, MA, USA) was used to verify and identify the chemical components of each sample. To prepare the samples for the FTIR spectra recordings, the different CS-g-MA molecules were dialyzed and lyophilized prior to spectral data collection. The IR spectra of the CS powder and MA solution were also recorded. The samples were placed on the diamond of the ATR-FTIR spectroscopy and their IR spectra were collected within the wavenumber range 4000–400 cm^{-1} at a resolution of 4 cm^{-1}. To ensure accuracy of the results, 16 scans were taken per run.

2.4 Mucoadhesive properties

A cone and plate viscometer (LAMY RHEOLOGY, France) was used to determine the mucoadhesive properties of CS-g-MA via the polymer's interaction with mucin glycoproteins. The samples were prepared by dissolving 20 mg CS and CS-g-MA in 1 mL acetic acid. Additionally, 0.5% w/v of mucin from porcine stomach (Sigma Aldrich, MO, USA) was prepared in a phosphate buffer solution with a pH of 7.4. The mucin solution and the polymer samples were mixed at a ratio of 1:1 by volume. The viscosity measurements were taken at a constant temperature of 25 ± 2 °C and a shear rate of 5 s^{-1}.

2.5 Cell viability test

MTT assays were used to determine cell viability using a modified method published by Pornpitchanarong et al. (2022). Briefly, normal human skin fibroblast (HNF) cells were cultured in DMEM supplemented with 1% penicillin-streptomycin and 10% fetal bovine serum (FBS) in an incubator under 5% CO_2 at 37 ± 2 °C. The cells were seeded in a 96-well plate at a density of 10,000 cells per well, then incubated overnight in a controlled environment. CS-g-MA was prepared at different concentrations between 312.5 and 2,500 µg/mL using the 2-fold dilution method in DMEM without serum. The cells were then incubated with CS-g-MA at different concentrations for 24 h. Next, the cells were washed with sterile phosphate-buffered saline (PBS; pH 7.4), then MTT solution (0.5 mg/mL) in DMEM with serum was added and incubated for 3 h. Afterwards, 100 µL dimethyl sulfoxide was used to dissolve the formazan crystals formed by the viable cells. Acetic acid (0.25% v/v) in DMEM was used as an untreated control. Absorbance was measured at 550 nm using a VICTOR NIVO™ multimode plate reader (PerkinElmer, US) and the relative percentage of viable cells was computed using Equation 2.

$$\% \text{ Cell viability} = \frac{\text{Absorbance of sample}}{\text{Absorbance of control}} \times 100 \qquad (2)$$

2.6 Antimicrobial test

2.6.1 Preparation of bacterial diluted solution

A colony of *S. aureus* and *E. coli* were subcultured separately in a nutrient broth, then incubated at 37 °C for 16–24 h. The bacterial suspension was diluted with nutrient broth to obtain bacteria concentrations of 1 × 10^8 and 1 × 10^6 CFU/mL by measuring optical density at 600 nm, with the McFarland standard used as a reference.

2.6.2 Preparation of fungal diluted solution

C. albicans was subcultured into Sabouraud dextrose broth, then incubated at 37 °C for 16–24 h. The fungal solution was then diluted with Sabouraud dextrose broth to adjust the fungal suspension concentration to 1 × 10^8 CFU/mL using the McFarland standard, which was monitored via optical density measurement. Finally, the fungal suspension was diluted to a concentration of 1 × 10^6 CFU/mL.

2.6.3 Minimum inhibitory concentration and minimum bacteriostatic concentration

The polymer samples were prepared by dissolving 20 mg CS and CS-g-MA powder in 1 mL 0.5% acetic acid. Then, the polymer solutions were diluted with the nutrient broth for the bacterial study and Sabouraud dextrose broth for the fungal study using a 2-fold dilution method to obtain sample concentrations of 2,500 µg/mL. Next, 10

μL of the bacterial and fungal suspensions were each added into 990 μL of the prepared polymer solution. The final concentration of bacterial and fungal suspensions was each 1×10^4 CFU/mL. The solution was incubated at 37 °C for 18 h. The minimum inhibitory concentration (MIC) was determined from the lowest concentration of the sample that produced a clear solution after incubation and was selected for the minimum bacteriostatic concentration (MBC) test. For the MBC test, 100 μL of the clear solution was spread onto the nutrient agar or Sabouraud dextrose agar for *C. albicans.* The agar was then incubated at 37 °C for 18 h. The MBC was determined to be the concentration of polymer that did not produce bacterial or fungal growth.

2.7 CS-g-MA tablet preparation

SFC is a hydrophilic fluorescent tracer used as a model drug in this study. Briefly, 100 mg CS-g-MA was ground and mixed with 1 mg SFC in a small mortar, then transferred to a tube and shaken for 1 min to ensure a uniform mixture. Next, 100 mg of the powder mixture was added to a hydraulic pestle with a diameter of 6.45 mm and compressed by a hydraulic manual press (Specac Ltd., UK) at 2 tons for 30 s. The resulting CS-g-MA tablet was used for the drug release test.

2.8 Drug release test

The drug release method used in this study was adapted from Pornpitchanarong et al. (2022). In brief, the CS-g-MA/SFC tablet was dissolved in PBS (pH 7.4) in a shaker incubator at 37 ± 2 °C at a shaking speed of 150 rpm and protected from light for 72 h. During the 72 h release test, 1 mL of medium was collected at predetermined time points for SFC analysis. An equivalent amount of fresh PBS was added back to the container to maintain a constant volume. The collected samples were placed in a 96-well plate and the fluorescence intensity of SFC was measured at the excitation and emission wavelengths of 485 and 535 nm, respectively, in a VICTOR NIVO™ multimode plate reader (PerkinElmer, US). A solution of the model drug (0.1% w/v) in a dialysis bag (6–8 kDa) was used as the control. The concentration of the model drug was calculated from the standard curve (10–1000 ng/mL; $R^2 > 0.999$). The cumulative amount of drug released was plotted against time.

2.9 Statistical analysis

The data were expressed as mean ± standard deviation. The student's t-test and one-way ANOVA followed by Tukey post hoc test were performed to determine significant differences at $p < 0.05$.

3. RESULTS AND DISCUSSION

3.1 CS-g-MA characterization

The CS-g-MA after freeze-drying was yellowish to white in color with a loose-fabric-like network. The percent yield of each synthesis is presented in Table 1. The CS:MA ratio of 3:4 provided a significantly higher yield than the other ratios ($p < 0.05$). The %DS of CS-g-MA was highest when the reaction was conducted at a CS:MA ratio of 3:4 (28.37%). This suggests that a ratio of 3:4 allows MA to be grafted onto the CS core structure. Thus, the 3:4 ratio was used to prepare CS-g-MA for the remaining experiments.

The NMR spectra (Figure 2) elucidated the structure of CS-g-MA. The signal of $-CH_3$ from the acetylated ring of chitosan occurred at a chemical shift of 2.0 ppm. The protons from the glucosamine ring ranged from 3.14 to 3.88 ppm. The signal from the MA spectrum occurred at a peak of 1.91 ppm, which was attributed to the $-CH_3$. Furthermore, the responses at 5.73 and 6.12 were the peaks of $=CH_2$ of the methacrylic moiety. The NMR signals of CS-g-MA corresponded to the spectra of both CS and MA with the $-CH_3$ of MA, $-CH_3$ of the CS acetylated ring, protons of the pyranose rings, at 1.88, 2.04, 3.15–3.88, and the vinyl protons at 5.67 and 6.06 ppm, respectively. These findings confirmed that CS-g-MA was successfully synthesized.

The characterization via the ATR-FTIR analyses of CS, MA, and CS-g-MA are shown in Figure 3. The CS absorption bands presented C–N stretching at 1026 cm^{-1}, C–H stretching at 2870 cm^{-1}, and O–H stretching at 3,361 cm^{-1}. MA showed O–H stretching at 3323 cm^{-1}, and C–H stretching at 2930 cm^{-1}. The CS-g-MA spectrum provided the CS spectrum with a new signal at 1632 cm^{-1} due to C=C stretching from MA. These findings indicate that MA was grafted onto the CS backbone.

The synthesis of CS-g-MA was confirmed to be successful through the ^{1}H-NMR and FTIR analyses of purified CS-g-MA. Li et al. (2015) synthesized a crosslinked CS and MA material through a chemically selective single-step process that involved acylating the amino group of CS with MA, without using coupling agents or catalysts. Anhydrides are highly reactive toward nucleophiles and are able to acylate the attacked nucleophile due to their reactivity. The reaction between an anhydride and an amine would thus form an amide through nucleophilic acyl substitution. During this reaction, the leaving group is removed from the anhydride and the amine loses a hydrogen, which allows a bond to form between the amine and the electrophilic carbonyl carbon. Thus, the synthesis of CS-g-MA was confirmed to be successful.

Table 1. The ratios of CS, MA, and % DS of CS-g-MA

Formulation	CS	MA	% DS	% Yield
1	1.5	4	22.12	41.86 ± 2.04
2	3	4	28.37	52.54 ± 0.59*
3	4.5	4	23.52	26.87 ± 0.61

Note: *Significant difference, $p < 0.05$

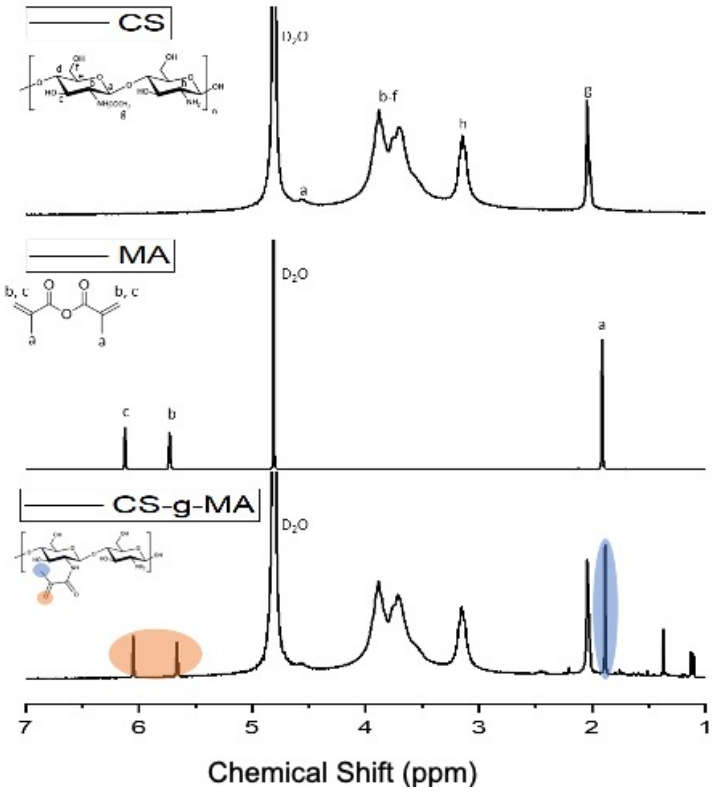

Figure 2. The ^{1}H-nuclear magnetic resonance spectroscopy (^{1}H-NMR) spectra of the CS, MA, and CS-g-MA

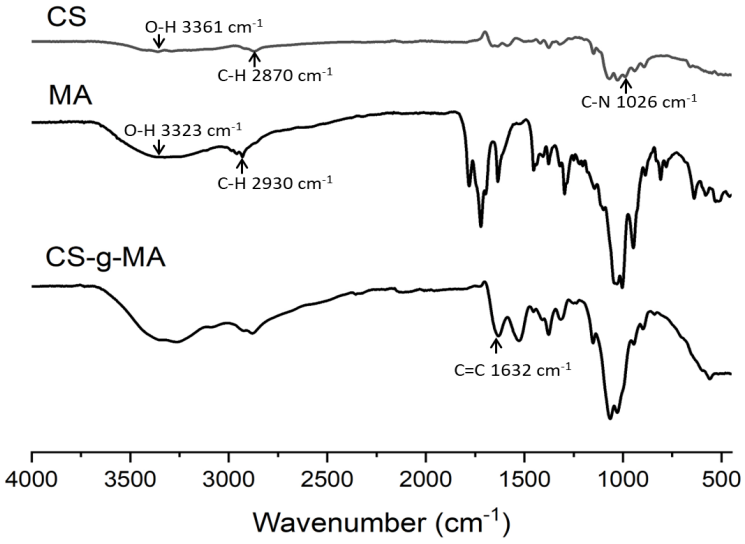

Figure 3. The attenuated total reflectance Fourier transform infrared spectroscopy (ATR-FTIR) spectra of the CS, MA, and CS-g-MA

3.2 Mucoadhesive properties

The mucoadhesive properties of CS-g-MA were evaluated and compared to those of CS via polymer-mucin interaction analysis. We examined the viscosity of CS, CS-g-MA, and their mixture with 0.5% mucin. The results are shown in a Table 2. The viscosity of the CS and CS-g-MA solutions were comparable, but the viscosity of the mixture increased significantly ($p < 0.05$) after the polymer was mixed with mucin. The increase in the viscosity at a low shear rate suggests a polymer-mucin interaction. The viscosity of CS + mucin increased by approximately double that of the CS solution alone, while the CS-g-MA improved 1.5-fold ($p < 0.05$). These results prove that the grafted methacrylate improved the mucoadhesive properties compared to the parent polymer. Collado-González et al. (2019) examined the

interaction between CS and mucin and found that the adhesion occurred through a combination of hydrogen bonding and electrostatic and hydrophobic interactions. In addition, the conjugation of MA onto CS may create stronger mucoadhesive properties through the covalent bonds that may occur between the methacrylate group and the thiols or other electrophilic groups of the mucin glycoprotein (Lam et al., 2021).

Table 2. The viscosity of the polymers and their mixtures with mucin indicating the polymer-mucin interaction.

Samples	Viscosity (cP)
Mucin	30.81 ± 1.12
CS	41.84 ± 3.69
CS-g-MA	42.59 ± 7.39
CS + mucin	87.67 ± 3.31#
CS-g-MA + mucin	100.39 ± 3.17*

Note: n = 3; # and * indicate significant differences from the solution; $p < 0.05$

3.3 Cell viability test

The biocompatibility of the synthesized polymers is presented in Figure 4. The prepared CS-g-MA were nontoxic to HNF cells, as indicated by the more than 80% cell viability found. This can be attributed to the biocompatibility of CS as a naturally-derived polymer. The performed chemical modification did not have a negative impact on the safety of the polymer. These results indicate that CS-g-MA has the potential to be used in biomedical applications.

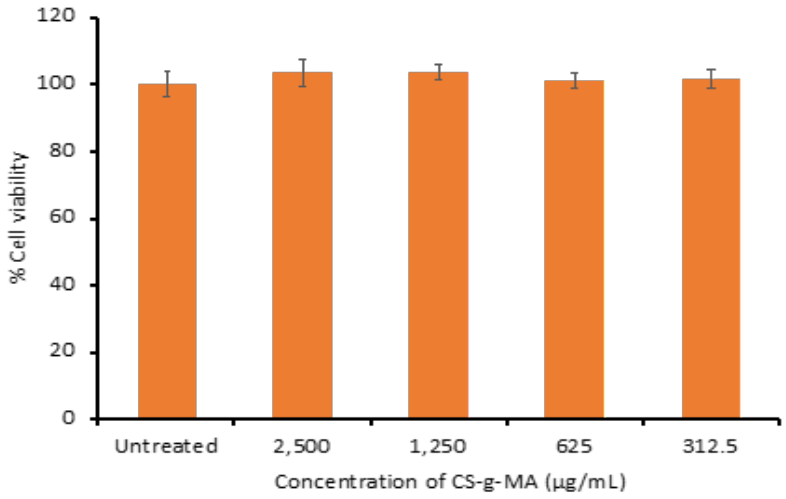

Figure 4. Cell viability of CS-g-MA at different concentrations after 24-h treatment (n = 5)

3.4 MIC & MBC

The MIC and MBC results of CS-g-MA are shown in Table 3. The positive controls (ciprofloxacin or fluconazole) were conducted at a concentration of 100 µg/mL. No microbial growth was observed in the positive controls, whereas the negative control of untreated cells showed microbial growth, which validates the experiments. CS-g-MA had greater antibacterial activities compared to those of CS against the tested gram-positive (*S. aureus*) and gram-negative (*E. coli*) bacteria and yeast (*C. albicans*). The improved antimicrobial effects may be due to its improved adhesion on the bacterial cell membranes and/or the effects on bacterial disruption, as suggested by other CS derivatives discussed in literature (Sahariah and Masson, 2017).

Table 3. The minimum inhibitory concentration (MIC) and minimum bactericidal concentration (MBC) of CS and CS-g-MA against *Staphylococcus aureus, Escherichia coli*, and *Candida albicans*

Samples	MIC (µg/mL)			MBC (µg/mL)		
	S. aureus	*E. coli*	*C. albicans*	*S. aureus*	*E. coli*	*C. albicans*
CS	156.25	625.00	2,500.00	156.25	1,250.00	2,500.00
CS-g-MA	39.06	312.50	1,250.00	39.06	625.00	2,500.00

3.5 Drug release

The release profile (Figure 5) of the model drug contained in the CS-g-MA tablet presented an extended profile with 50%–60% drug release during a 24–72 h period. The rapid release rate at the initial stage was attributed to the hydrophilic nature of SFC that freely diffused through the dialysis membrane (Rangsimawong et al., 2014). The SFC solution did not completely release from the dialysis bag

because release from the bag required a high concentration gradient to provide sufficient osmotic pressure. The release at 72 h indicated that most of the drug was released. Thus, some drug content may be unable to pass through the membrane, which leads to a slightly lower release rate. However, the CS-g-MA tablet may also swell in the release medium, which could also result in a declined release rate. Thus, the release profile of the hydrophilic drug from the mucoadhesive tablet was in a biphasic manner. Moreover, the profiles of SFC release in the medium were fitted in the kinetic models of zero order, first order, and Higuchi's model. The highest linear regression (R^2) represents the best-fit model for each release profile. As shown in Table 4, SFC release through the dialysis bag followed the first-order model, since the concentration gradient affected the release through the membrane. That is, the drug concentration impacted the release rate. This was best described by the kinetic model. On the other hand, the release of SFC from the tablet best fit the Higuchi's model because the release of the drug had to go through a swollen drug matrix that retarded the release rate of the drug. These findings demonstrate that the polymer could be used in a drug delivery system or acquired as a drug delivery platform for controlled release drug delivery (Dash et al., 2010; Heredia et al., 2022).

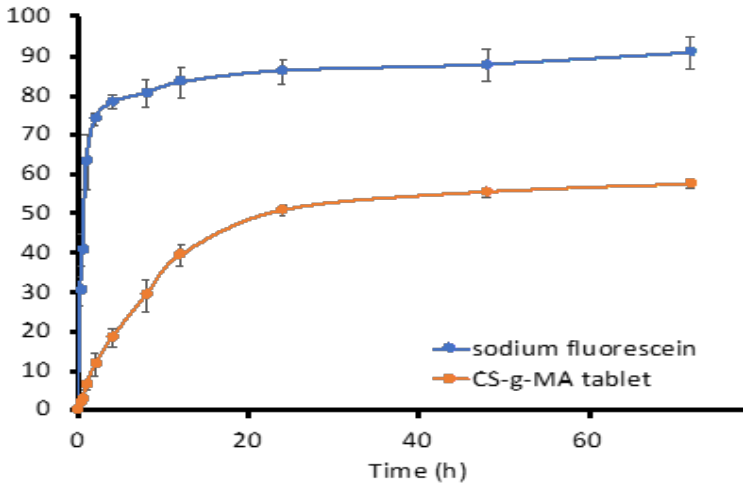

Figure 5. The release profile of the model drug from the CS-g-MA tablet and control (sodium fluorescein in an aqueous solution; n = 3)

Table 4. Drug release kinetic model represented by the R^2 of the linear release profile

Samples	Zero order	First order	Higuchi
SFC solution	0.4836	0.9919	0.6481
SFC in CS-g-MA tablet	0.9773	0.6591	0.9873

4. CONCLUSION

The CS-g-MA polymer was successfully synthesized using CS and MA at a weight ratio of 3:4, which resulted in a maximum degree of substitution of 28%. The CS derivative improved its mucoadhesive properties, with a greater effectiveness in inhibiting and killing bacteria and fungi compared to regular CS. The synthesized CS derivative was also found to be non-toxic to human skin cells. As demonstrated by the prolonged release profile of its tablet formulation, the CS-g-MA polymer may be useful in drug delivery. Overall, CS-g-MA has potential for use as a drug delivery system with enhanced mucoadhesive properties and antimicrobial activities compared to CS.

ACKNOWLEDGMENT

We would like to acknowledge the financial support received through the PhD Student Scholarship by the Faculty of Pharmacy, Silpakorn University.

REFERENCES

Aranaz, I., Alcantara, A. R., Civera, M. C., Arias, C., Elorza, B., Heras Caballero, A., and Acosta, N. (2021). Chitosan: An overview of its properties and applications. *Polymers (Basel)*, 13(19), 3256.

Bernkop-Schnürch, A., and Dünnhaupt, S. (2012). Chitosan-based drug delivery systems. *European Journal of Pharmaceutics and Biopharmaceutics*, 81(3), 463–469.

Collado-González, M., González Espinosa, Y., and Goycoolea, F. M. (2019). Interaction between chitosan and mucin: fundamentals and applications. *Biomimetics (Basel)*, 4(2), 32.

Das, S. S., Kar, S., Singh, S. K., Verma, P. R. P., Hussain, A., and Beg, S. (2022). Chapter 2—Chitosan-based systems for oral drug delivery applications. In *Chitosan in Drug Delivery* (Hasnain, M. S., Beg, S., and Nayak, A. K., Eds.), pp. 23–53. Cambridge: Academic Press.

Dash, S., Murthy, P. N., Nath, L., and Chowdhury, P. (2010). Kinetic modeling on drug release from controlled drug

delivery systems. *Acta Poloniae Pharmaceutica*, 67(3), 217–223.

Deusenbery, C., Wang, Y., and Shukla, A. (2021). Recent innovations in bacterial infection detection and treatment. *ACS Infectious Diseases*, 7(4), 695–720.

Heredia, N. S., Vizuete, K., Flores-Calero, M., Pazmino, V. K., Pilaquinga, F., Kumar, B., and Debut, A. (2022). Comparative statistical analysis of the release kinetics models for Nanoprecipitated drug delivery systems based on Poly(lactic-co-glycolic acid). *PLoS One*, 17(3), e0264825.

Ke, C. L., Deng, F. S., Chuang, C. Y., and Lin, C. H. (2021). Antimicrobial actions and applications of chitosan. *Polymers (Basel)*, 13(6), 904.

Kenawy, E.-R., Abdel-Hay, F. I., El-Magd, A. A., and Mahmoud, Y. (2016). Biologically active polymers: Modification and anti-microbial activity of chitosan derivatives. *Journal of Bioactive and Compatible Polymers*, 20(1), 95–111.

Kolawole, O. M., Lau, W. M., and Khutoryanskiy, V. V. (2018). Methacrylated chitosan as a polymer with enhanced mucoadhesive properties for transmucosal drug delivery. *International Journal of Pharmaceutics*, 550(1–2), 123–129.

Kongkaoroptham, P., Piroonpan, T., and Pasanphan, W. (2021). Chitosan nanoparticles based on their derivatives as antioxidant and antibacterial additives for active bioplastic packaging. *Carbohydrate Polymers*, 257, 117610.

Kumar, M. N. V. R., Muzzarelli, R. A. A., Muzzarelli, C., Sashiwa, H., and Domb, A. J. (2004). Chitosan chemistry and pharmaceutical perspectives. *Chemical Reviews*, 104(12), 6017–6084.

Lam, H. T., Zupančič, O., Laffleur, F., and Bernkop-Schnürch, A. (2021). Mucoadhesive properties of polyacrylates: Structure—function relationship. *International Journal of Adhesion and Adhesives*, 107, 102857.

Li, B., Wang, L., Xu, F., Gang, X., Demirci, U., Wei, D., Li, Y., Feng, Y., Jia, D., and Zhou, Y. (2015). Hydrosoluble, UV-crosslinkable and injectable chitosan for patterned cell-laden microgel and rapid transdermal curing hydrogel *in vivo*. *Acta Biomater*, 22, 59–69.

Matica, M. A., Aachmann, F. L., Tondervik, A., Sletta, H., and Ostafe, V. (2019). Chitosan as a wound dressing starting material: Antimicrobial properties and mode of action. *International Journal of Molecular Sciences*, 20(23), 5889.

Cankaya, N. (2019). Grafting of chitosan: Structural, thermal and antimicrobial properties. *Journal of the Chemical Society of Pakistan*, 41(2), 240–245.

Pornpitchanarong, C., Rojanarata, T., Opanasopit, P., Ngawhirunpat, T., Bradley, M., and Patrojanasophon, P. (2022). Maleimide-functionalized carboxymethyl cellulose: A novel mucoadhesive polymer for transmucosal drug delivery. *Carbohydrate Polymers*, 288, 119368.

Rangsimawong, W., Opanasopit, P., Rojanarata, T., and Ngawhirunpat, T. (2014). Terpene-containing PEGylated liposomes as transdermal carriers of a hydrophilic compound. *Biological and Pharmaceutical Bulletin*, 37(12), 1936–1943.

Sahariah, P., and Masson, M. (2017). Antimicrobial chitosan and chitosan derivatives: a review of the structure-activity relationship. *Biomacromolecules*, 18(11), 3846–3868.

Shanmugam, A., Kathiresan, K., and Nayak, L. (2016). Preparation, characterization and antibacterial activity of chitosan and phosphorylated chitosan from cuttlebone of *Sepia kobiensis* (Hoyle, 1885). *Biotechnology Reports*, 9, 25–30.

Shariatinia, Z. (2019). Pharmaceutical applications of chitosan. *Advances in Colloid and Interface Science*, 263, 131–194.

Siti Zuhairah, Z., and Khuriah Abdul, H. (2021). Chitosan-based oral drug delivery system for peptide, protein and vaccine delivery. In *Chitin and Chitosan - Physicochemical Properties and Industrial Applications* (Berrada, M., Ed.), pp. 1–22. London: IntechOpen.

Sogias, I. A., Khutoryanskiy, V. V., and Williams, A. C. (2010). Exploring the factors affecting the solubility of chitosan in water. *Macromolecular Chemistry and Physics*, 211(4), 426–433.

Wang, H., Bu, X., Huang, Z., Yang, J., and Qiu, T. (2014). Synthesis of methacrylic anhydride by batch reactive distillation: Reaction kinetics and process. *Industrial & Engineering Chemistry Research*, 53(44), 17317–17324.

Wang, W., Meng, Q., Li, Q., Liu, J., Zhou, M., Jin, Z., and Zhao, K. (2020). Chitosan derivatives and their application in biomedicine. *International Journal of Molecular Sciences*, 21(2), 487.

Xing, K., Zhu, X., Peng, X., and Qin, S. (2014). Chitosan antimicrobial and eliciting properties for pest control in agriculture: A review. *Agronomy for Sustainable Development*, 35(2), 569–588.

Yu, L. M., Kazazian, K., and Shoichet, M. S. (2007). Peptide surface modification of methacrylamide chitosan for neural tissue engineering applications. *Journal of Biomedical Materials Research Part A*, 82(1), 243–255.